PCCP

ROYAL SOCIETY OF CHEMISTRY

PAPER

View Article Online
View Journal | View Issue

Cite this: *Phys. Chem. Chem. Phys.*, 2025, **27**, 13735

Common mechanism of dual emission in linearly-linked donor–acceptor-type thermally activated delayed fluorescence molecules†

Tomohiro Ryu,[a] Arvydas Ruseckas,[b] Masaki Saigo,[a] Kiyoshi Miyata,[a] Youichi Tsuchiya,[c] Hajime Nakanotani,[c] Chihaya Adachi,[c] Ifor D. W. Samuel[b] and Ken Onda *[a]

Linearly-linked donor–acceptor-type (D–A) thermally activated delayed fluorescence molecules have been expected to be used as efficient emitters in organic light emitting diodes. Despite their simple molecular structures, some of these molecules exhibit a complex dual emission mechanism due to their two conformers: quasi-coplanar (q-copl.) and perpendicular (perp.) conformers. We have investigated three molecules of this type: phenothiazine–triphenyltriazine, 9,9-dimethyl-9,10-dihydroacridine–triphenyltriazine, and phenoxazine–triphenyltriazine using picosecond time-resolved photoluminescence and femtosecond transient absorption spectroscopy measurements. We have revealed the dual emission mechanism common to the three molecules: after photoexcitation, in the q-copl. conformer, the second singlet excited state with local excitation character emits strong fluorescence, which decays in 3–7 ps as it relaxes to the lowest singlet excited state with charge transfer (CT) character. The CT state exhibits relatively weak fluorescence with a lifetime of tens to hundreds of picoseconds. In the perp. conformer, the excited state shows a pronounced CT character with a weaker oscillator strength reduced by two orders of magnitude, structural relaxation in about 4 ps and a slow decay in >1 ns. The dual emission intensity ratio is determined by the population ratio between the q-copl. and perp. conformers in the ground state. The difference in this intensity ratio between the three molecules is ascribed to the difference in relative energetic stability between the two conformers in the ground state. The emission mechanism common to the linearly-linked D–A molecules deepens the understanding of their photophysical properties and opens new pathways for the development of advanced photofunctional materials.

Received 30th March 2025,
Accepted 3rd June 2025

DOI: 10.1039/d5cp01226k

rsc.li/pccp

Introduction

Organic molecules that possess charge transfer (CT) excited states have recently attracted attention as promising materials for organic electronic devices. In these molecules, charge distribution within or between molecules is significantly localized by electronic transitions and the spatially separated transition orbitals lead to various functions. For example, thermally activated delayed fluorescence (TADF) arising from the small energy gap between singlet and triplet states in the CT excited states is used in organic light-emitting diodes (OLEDs).[1–4] Near-infrared emission from the CT excited state with a large Stokes shift is used in bioimaging.[5–7] Intermolecular CT excited states are used in organic photovoltaics.[8,9] The simplest strategy to create molecules possessing CT excited states is to link electron donor and acceptor molecules by carbon single bonds, enabling intramolecular CT in the excited states, referred to as linearly-linked D–A molecules. The advantage of this type of molecule is that diverse functions can be easily achieved by appropriate selection of donor and acceptor molecules.

Some linearly-linked D–A molecules exhibit dual emission caused by two emissive conformers in the excited state.[10–12] Typical examples are a series of molecules bearing a phenothiazine (PTZ) as a donor.[13–16] Tanaka *et al.* first reported a PTZ-donor D–A molecule exhibiting dual emission, using triphenyltriazine (TRZ) as the acceptor, named **PTZ–TRZ** (Fig. 1a).[17] This molecule has two types of conformers in the excited state, a quasi-coplanar (q-copl.) or quasi-axial conformer (Fig. 1d), in

[a] *Department of Chemistry, Faculty of Science, Kyushu University, 744 Motooka, Nishi, Fukuoka 819-0395, Japan. E-mail: konda@chem.kyushu-univ.jp*
[b] *Organic Semiconductor Centre, School of Physics and Astronomy, University of St Andrews, North Haugh, St Andrews, Fife, KY16 9SS, UK*
[c] *Center for Organic Photonics and Electronics Research, Kyushu University, 744 Motooka, Nishi, Fukuoka 819-0395, Japan*

† Electronic supplementary information (ESI) available. See DOI: https://doi.org/10.1039/d5cp01226k

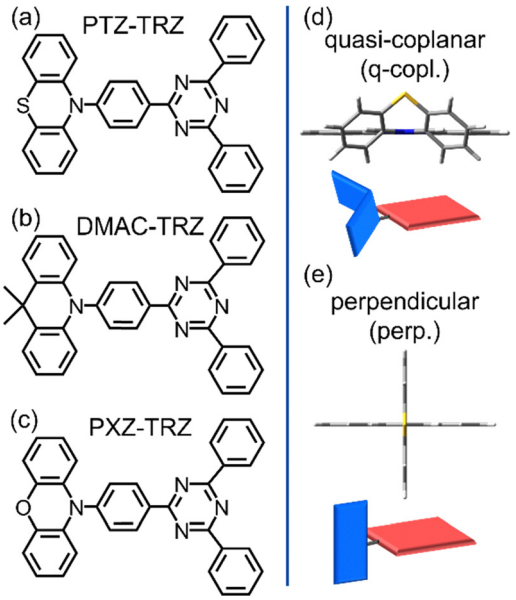

Fig. 1 (a)–(c) Molecular structures of (a) **PTZ–TRZ**, (b) **DMAC–TRZ**, and (c) **PXZ–TRZ**. (d) and (e) Geometries and schematic diagrams of the two conformers of **PTZ–TRZ**: (d) quasi-coplanar and (e) perpendicular conformers.

which the bent donor and acceptor are arranged horizontally, and a perpendicular (perp.) or quasi-equatorial conformer (Fig. 1e), in which the planner donor and planar acceptor are arranged perpendicularly. This is attributed to the bending of the PTZ plane and the flexible dihedral angle between the donor and acceptor. They found that each emission originates from a different CT excited state and has different photophysical properties: only the perp. conformer exhibits TADF. D–A molecules analogous to **PTZ–TRZ** also exhibit dual emission from two conformers. Stavrou *et al.* demonstrated that 9,9-dimethyl-9,10-dihydroacridine–TRZ (**DMAC–TRZ**, Fig. 1b), which had not been previously discussed in the context of dual emission, exhibits dual emission and similar emission properties to **PTZ–TRZ** through a comprehensive investigation.[18]

Linearly-linked D–A molecules exhibiting dual emission have complex excited-state dynamics due to their two flexible conformers. Understanding the complex dynamics arising from the simple structure is important not only for their applications but also for fundamental photophysics. For **PTZ–TRZ**, Chen *et al.* investigated the conformational change between the two conformers from the time profile of each emission on the picosecond timescale and determined its time constant to be 1.8 ps in cyclohexane solution.[19] We investigated the excited state dynamics of **PTZ–TRZ** and their solvent dependence by time-resolved measurements.[20] The time-resolved photoluminescence (TR-PL) measurements revealed that the q-copl. conformer exhibited emission from a higher singlet excited state. The measurements also revealed that the photophysical properties of the two structures respond differently to the polarity of the solvent: a shorter emission lifetime and no TADF in high dielectric permittivity solution in the perp. conformer, and no significant solvent dependence in the q-copl. conformer. The visible transient absorption (TA) measurements revealed that the structural change from the q-copl. to perp. conformers occurs with the time constant of approximately 8 ps. For **DMAC–TRZ**, Franca *et al.* demonstrated the picosecond behavior of the excited state and its solvent dependence.[21] The TA measurements revealed that the structural change from the q-copl. conformer to the perp. conformer occurs within 20 ps in cyclohexane solution, while solvation occurs within 17 ps in toluene solution. These previous studies suggest that the excited-state dynamics of linearly-linked D–A molecules involve complex picosecond dynamics; however, no spectra of each emission have been observed on the picosecond timescale, leading to an incomplete understanding of the detailed dynamics. Moreover, these investigations focused on specific molecules; thus, the comprehensive dynamics common to more D–A molecules remain unexplored.

In order to explore the common excited-state dynamics in linearly-linked D–A molecules on the picosecond timescale, we have investigated three prototypical molecules: **PTZ–TRZ** and **DMAC–TRZ**, which are typical molecules exhibiting dual emission, and phenoxazine–TRZ (**PXZ–TRZ**, Fig. 1c) as an analogue using picosecond TR-PL and femtosecond TA spectroscopies. We found that all three molecules exhibit dual emission originating from the two conformers, q-copl. and perp. After photoexcitation, in the q-copl. conformer, the second singlet excited (S_2) state with localized excitation (LE) character emits strong fluorescence with a lifetime of 3–7 ps and simultaneously relaxes to the lowest singlet excited state (S_1) with CT character, which exhibits weak fluorescence with a lifetime of tens to hundreds of picoseconds. In the perp. conformer, the structural relaxation in the S_1 state with CT character occurs with a lifetime of 4 ps and then the S_1 state after the relaxation exhibits long-lived fluorescence. The relative emission intensity between the q-copl. and perp. conformers is determined by the stability of the q-copl. conformer in the ground (S_0) state. The results propose a new energy diagram and emission mechanism that would be common to similar linearly-linked D–A molecules.

Experimental

Sample preparation

PTZ–TRZ, **DMAC–TRZ**, and **PXZ–TRZ** were synthesized as described in the previous study.[17,22,23]

Steady-state PL spectroscopy and UV-vis absorption spectroscopy

Steady-state photoluminescence (PL) spectra were measured using a spectrofluorometer (JASCO FP-8300). UV-vis absorption spectra were obtained with a spectrophotometer (JASCO V-780). The samples for the steady-state PL and UV-vis absorption measurements were prepared using 0.1 mM and 0.01 mM toluene solution, respectively.

TR-PL spectroscopy

The TR-PL spectra were measured using a streak camera system (Hamamatsu C6860, response function: 2 ps). The samples

were excited by a third harmonic (343 nm) of the output of a Yb:KGW regenerative amplifier (Light Conversion PHAROS, central wavelength: 1030 nm, pulse duration: 200 fs) at a pulse repetition rate of 100 kHz. The optical path length of the solution cell was 1 cm. The measurements were conducted while stirring the solution to avoid damage to the sample. All samples were prepared using 0.1 mM toluene or dichloromethane (DCM) solution. The obtained TR-PL spectra were analyzed by the global analysis using Glotaran.[24]

Femtosecond TA spectroscopy

The femtosecond TA measurements were performed using home-built pump–probe setups. The Yb:KGW regenerative amplifier at a pulse repetition rate of 1 kHz (pulse energy: 1 mJ per pulse) was used as the light source. The output pulse was split into two optical paths using a beam splitter. One of the split outputs was fed into an optical parametric amplifier (OPA, Light Conversion ORPHEUS), where the output wavelength was tuned to 740 nm, 720 nm, and 690 nm. Each light beam was converted using a β-BaB_2O_4 (BBO) crystal to its second harmonic at 370 nm (for **DMAC–TRZ**), 360 nm (for **PTZ–TRZ**), and 345 nm (for **PXZ–TRZ**), respectively, and used as pump pulses. The other output was focused on a sapphire crystal (3 mm in thickness), generating white light from 500 to 950 nm, which was used as the probe pulse. The magic angle (∼54.7°) was adopted between the pump and probe polarizations. The probe pulse that passed through the sample was dispersed by a polychromator (JASCO CT-10, 300 grooves/500 nm) and detected using a multichannel CMOS sensor-based system (UNISOKU USP-PSMM-NP). The pump pulse fluence at the sample position was 0.31 mJ cm^{-2} for **PTZ–TRZ**, 0.23 mJ cm^{-2} for **DMAC–TRZ**, and 0.20 mJ cm^{-2} for **PXZ–TRZ**. All samples were prepared using 0.1 mM toluene solution in a 1 mm cell. The obtained TA spectra were analyzed by the global analysis using Glotaran.[24]

Quantum chemical calculations

Quantum chemical calculations were performed using the Gaussian 16 C.01 package.[25] The S_0 state was calculated based on density functional theory (DFT), and the singlet excited states were calculated based on time-dependent (TD)-DFT. The solvent effect was examined by using the polarizable continuum model of toluene solution (dielectric constant: 2.38). We employed the 6-31G(d,p) basis set and B3LYP functional.

Results and discussion

Steady-state photophysical properties

Fig. 2a shows the UV-vis absorption and PL spectra of **PTZ–TRZ**, **DMAC–TRZ**, and **PXZ–TRZ** in toluene solution. The extinction coefficient of **PTZ–TRZ** in the low energy absorption band with a peak at 350 nm is about twice higher than those in the other two molecules. All the PL spectra show dual emission at 409 nm and 580 nm for **PTZ–TRZ**, at 413 nm and 500 nm for **DMAC–TRZ**, and at 409 nm and 560 nm for **PXZ–TRZ** (Fig. 2b). The PL quantum yields in toluene solution for **PTZ–TRZ**, **DMAC–TRZ**, and **PXZ–TRZ** are 20%, 79%, and 30%, respectively.[20,22,26]

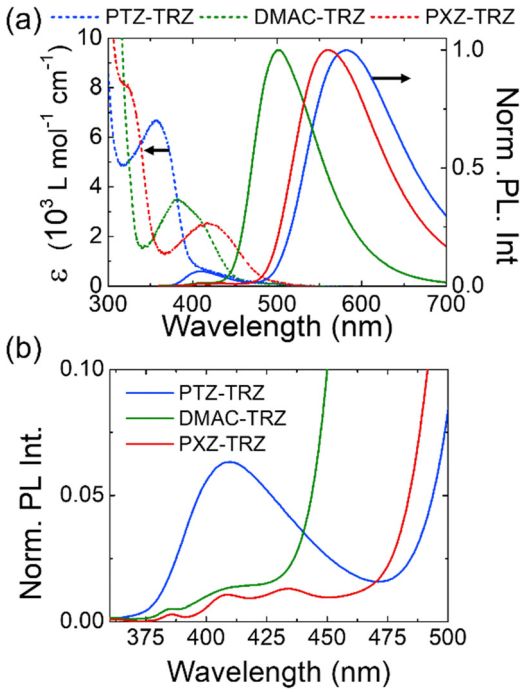

Fig. 2 (a) The UV-vis absorption spectra (dashed lines) and the normalized PL spectra (solid lines) of **PTZ–TRZ** (blue), **DMAC–TRZ** (green), and **PXZ–TRZ** (red) in toluene solution. The concentration of the solutions for PL measurements is 0.1 mM. (b) Expanded normalized steady-state PL spectra in the range of 360–500 nm.

The dual emissions observed for **PTZ–TRZ** and **DMAC–TRZ** are consistent with the previous reports, whereas that for **PXZ–TRZ** is newly observed. To confirm this, we conducted concentration-dependent steady-state PL measurements for the three D–A molecules in 0.01 mM, 0.1 mM, and 1 mM toluene solutions (Fig. S1–S3, ESI†). Note that the decrease of the relative intensity of the peak in the short-wavelength range with increasing concentration for **DMAC–TRZ** and **PXZ–TRZ** is attributed to self-absorption owing to a large overlap between the absorption and emission spectra in the short-wavelength range as shown in Fig. 2a.

According to the previous studies on **PTZ–TRZ** and **DMAC–TRZ**, the emission in the short-wavelength range is assigned to the emission from the q-copl. conformer.[17–21] Thus, this result indicates that all three molecules have both q-copl. and perp. conformers in the excited state.

TR-PL spectra in the picosecond range

To explore the emission mechanism at the earliest stage, we conducted TR-PL measurements with a time resolution of ∼1 ps. Fig. 3a–c shows the TR-PL spectra of **PTZ–TRZ**, **DMAC–TRZ**, and **PXZ–TRZ**, respectively. In this time region, all the molecules clearly exhibit dual emission at 410 nm and 557 nm in **PTZ–TRZ**, at 406 nm and 497 nm in **DMAC–TRZ**, and at 400 nm and 543 nm in **PXZ–TRZ**. Because the shorter

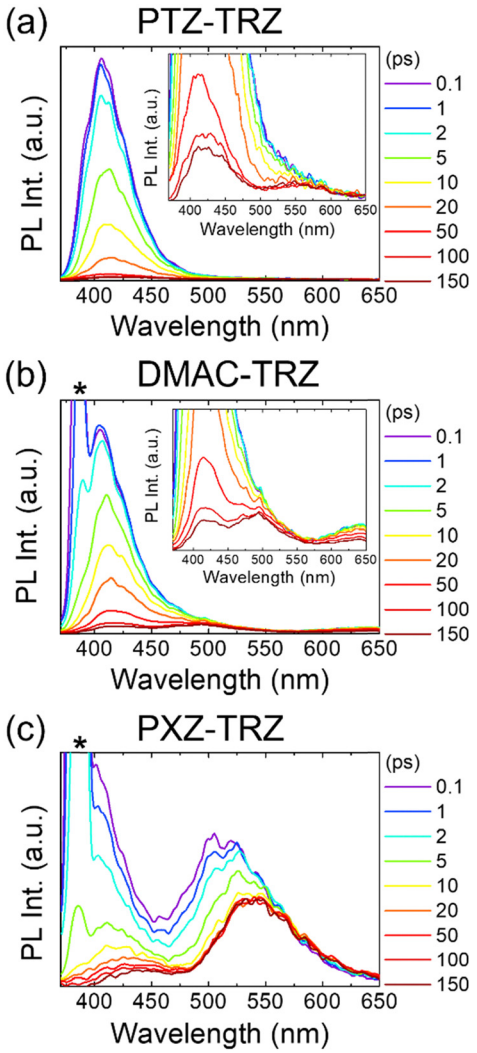

Fig. 3 The TR-PL spectra on the picosecond timescale of (a) **PTZ–TRZ**, (b) **DMAC–TRZ**, and (c) **PXZ–TRZ** in toluene solution. Insets of (a) and (b) show the enlarged TR-PL spectra in the range of 375–650 nm. The asterisk represents the Raman scattering signal.

wavelength emission peaks in the spectra at 0.1 ps and 150 ps for all the molecules resemble those in the steady-state PL spectra (a comparison of the normalized spectra is shown in Fig. S4, ESI†), we assigned these peaks to the emission from the q-copl. conformer. Based on our previous report, the slight red shift from 0.1 ps to 150 ps (Fig. S5, ESI†) is attributed to the internal conversion from a higher singlet excited state to the S_1 state of the q-copl. conformers associated with vibrational relaxation and solvation. In the emission of the perp. conformer, the red shift was observed in **PXZ–TRZ,** while it was not observed in the other molecules because the emission is overlapped by the shoulder of the emission from the q-copl. conformer. Unlike the emissions from the q-copl. conformers, the changes in the emission intensity of the perp. conformers were small. In addition, the finding that the maximum intensities of emission appear immediately after photoexcitation (at 0.1 ps) for both conformers indicates that the two conformers are excited simultaneously for all the molecules.

Origin of the emission immediately after photoexcitation

To clarify the origin of the emission immediately after photoexcitation, accompanied by a red shift in both conformers, we calculated the oscillator strengths between the S_1 to S_5 states and the S_0 state in the q-copl. and perp. conformers for the three molecules using the optimized structure of the S_1 state and the values are summarized in Table 1. In the q-copl. conformer, the oscillator strengths of the S_1 state for the three molecules were almost zero, while those of the S_2 state were 0.74, 0.78, and 0.67 for **PTZ–TRZ**, **DMAC–TRZ**, and **PXZ–TRZ**, respectively. Thus, the strong emission from the q-copl. conformer immediately after photoexcitation is attributed to the emission from the S_2 state. To estimate the absorption spectra, the oscillator strengths of the same transitions were calculated using the optimized structure of the S_0 state (Table S1, ESI†). As a result, the oscillator strengths of the S_1 state were almost zero, while those of the S_2 state were approximately 0.9 for the three molecules, indicating that the absorption peak of the q-copl. conformer is assigned to the transition to the S_2 state for each molecule.

Based on the calculated NTOs (natural transition orbitals) shown in Fig. S8, S10 and S12 (ESI†), the large oscillator strength in the S_2 state arises from the large overlap between hole and electron orbitals associated with the transition. This means that the S_2 state is dominated by LE character ($^1LE_{q\text{-}copl.}$ state). In contrast, the S_1 state has a prominent CT character ($^1CT_{q\text{-}copl.}$ state) as indicated by the small overlap between hole and electron orbitals. Because the energies of the S_2 and S_1 states are close as shown in Fig. S6 (ESI†), these singlet excited states are expected to acquire mixed LE–CT character. This is consistent with the quantum chemical calculations presented by Stavrou *et al.* for **DMAC–TRZ**.[18] In the perp. conformer, the oscillator strengths of the three molecules were almost zero primarily due to the small overlap of its transition orbitals (Fig. S9, S11, and S13, ESI†). We concluded from these results that the initial emission from the perp. conformer is assigned to the S_1 state dominated by CT character ($^1CT_{perp.}$ state). The redshift of this emission, which appears prominently for **PXZ–TRZ**, is presumably ascribed to the structural relaxation in the $^1CT_{perp.}$ state. Note that the emission from the perp. conformer is attributed to the emission from a slightly twisted structure caused by fluctuations in the dihedral angle between the donor–acceptor, as previously reported for **DMAC–TRZ**.[26]

Table 1 The calculated oscillator strength (*f*) of the S_1 to S_5 states in each conformer of each molecule. All values were calculated with the optimized structure of the S_1 state

f (S_1 state)		S_1	S_2	S_3	S_4	S_5
PTZ–TRZ	q-copl.	0	0.74	<0.01	0	<0.01
	perp.	0	0	<0.01	0	0
DMAC–TRZ	q-copl.	0	0.78	0	0.10	0.25
	perp.	0	0	<0.01	<0.01	0
PXZ–TRZ	q-copl.	0	0.67	<0.01	<0.01	0.21
	perp.	0	0	<0.01	<0.01	0

Time constants of the relaxation processes

We estimated the time constants of the fast processes in the emission mechanism using the global analysis for the TR-PL spectra. The global analysis was performed in the wavelength region corresponding to the emission of the q-copl. conformer within the dual emission: 370–480 nm in **PTZ–TRZ**, 395–450 nm in **DMAC–TRZ**, and 398–460 nm in **PXZ–TRZ**. Note that, in the case of **DMAC–TRZ** and **PXZ–TRZ**, the wavelength region of Raman scattering was not included in the analysis: 370–395 nm in **DMAC–TRZ** and 370–398 nm in **PXZ–TRZ**. We performed the analysis using a sequential two-state model for the emission of the q-copl. conformer assuming that two evolution associated spectra (EAS1 and EAS2) are assigned to the $^1LE_{q\text{-copl.}}$ and $^1CT_{q\text{-copl.}}$ states, respectively (Fig. S14, ESI†). These results are shown in Fig. 4 and the values are summarized in Table S2 (ESI†). In **PTZ–TRZ**, the time constant of EAS1 (τ_{EAS1}) was estimated to be 5.2 ps (Fig. 4a and b). Considering that the $^1LE_{q\text{-copl.}}$ state exhibits strong emission, this time constant is attributed to a relaxation process from the $^1LE_{q\text{-copl.}}$ state to the $^1CT_{q\text{-copl.}}$ state including vibration relaxation and solvation. For **DMAC–TRZ** and **PXZ–TRZ**, the τ_{EAS1} values were estimated to be 6.8 ps (Fig. 4c and d) and 3.4 ps (Fig. 4e and f), respectively.

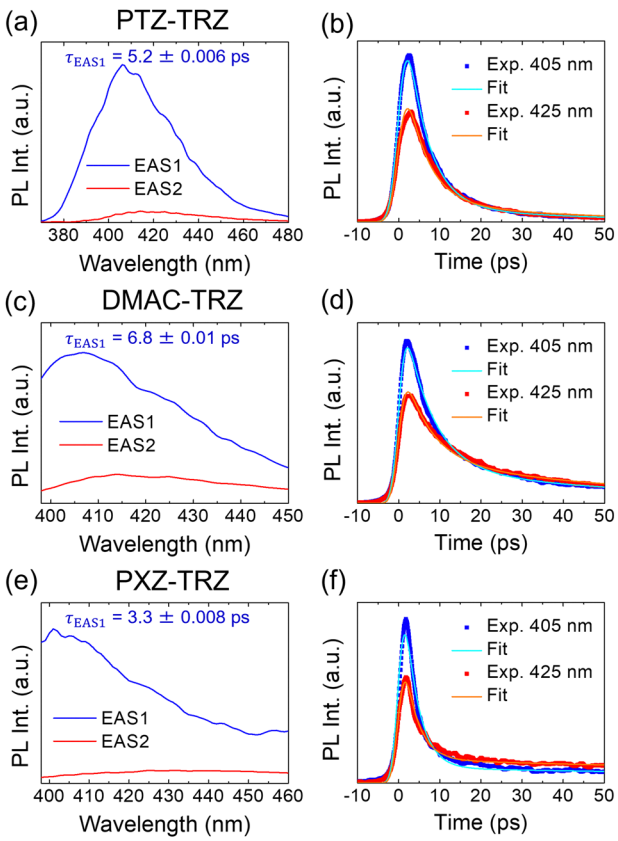

Fig. 4 The results of a global analysis of the TR-PL spectra. The evolution associated spectra (EAS) of (a) **PTZ–TRZ**, (c) **DMAC–TRZ**, and (e) **PXZ–TRZ**. Comparison of the time profiles at 405 and 425 nm of the TR-PL spectra to the fitting of a global analysis in (b) **PTZ–TRZ**, (d) **DMAC–TRZ**, and (f) **PXZ–TRZ**. We used a sequential two-state model for all the molecules.

These results indicate that the q-copl. conformer for all three molecules has the same emission mechanism: immediately after photoexcitation, the $^1LE_{q\text{-copl.}}$ state emits strong fluorescence, which decays in 3–7 ps as it acquires CT character. It should be noted that since the emission from the q-copl. conformer had not fully decayed within the experimental time window up to 150 ps, the estimated time constants of EAS2 (τ_{EAS2}) do not accurately represent the lifetime of the emission from the $^1CT_{q\text{-copl.}}$ state.

The global analysis was also performed for the emission of **PXZ–TRZ** in the wavelength region corresponding to the emission of the perp. conformer within the dual emission (480–652 nm). We performed the analysis using the same model of the emission of the q-copl. conformer assuming that EAS1 and EAS2 are assigned to the $^1CT_{q\text{-copl.}}$ states before and after structural relaxation, respectively (Fig. S14, ESI†). The results are shown in Fig. S15 and Table S2 (ESI†). The τ_{EAS1} was estimated to be 4.0 ps, indicating that the structural relaxation in the $^1CT_{perp.}$ state occurs at 4 ps. The τ_{EAS2} was longer than the time window, which was assigned to the fluorescence of the $^1CT_{perp.}$ state after relaxation. For the other molecules, the global analysis for the emission of the perp. conformer was not performed because the emission of the perp. conformer immediately after photoexcitation was largely overlapped by the shoulder of the emission of the q-copl. conformer. However, the structural relaxation with a time constant similar to that of **PXZ–TRZ** may also occur in the other molecules.

Since the fluorescence of CT states is highly sensitive to the polarity of the solvent, TR-PL measurements of the q-copl. conformer were conducted in DCM, which has a much higher dielectric permittivity (ε = 9.1) compared to toluene (ε = 2.38) (Fig. S16, ESI†). Global analysis of the TR-PL spectra in DCM was performed in the same manner as in toluene solution and the fast decay component was determined to be 2–3 ps for all three molecules. This result indicates that the relaxation process from the LE state to the CT state in the q-copl. conformer is accelerated in the solvent of higher dielectric permittivity. A similar trend has been observed in molecules with twisted intramolecular charge transfer (TICT) in the excited state and is reported to be due to the stabilization of the CT state, which makes the potential energy surface steeper and the activation barrier from the LE to CT state smaller.[27]

Intensity ratios of the dual emission

Although the three molecules have almost the same time constant for their respective emissions, the intensity ratios and the time evolutions of the dual emission ratio are significantly different. In **PTZ–TRZ**, the emission ratio of the q-copl. conformer to the perp. conformer, $I_{E,q\text{-copl.}}/I_{E,perp.}$, was estimated to be approximately 141 immediately after photoexcitation and it decreased to 2.8 at 150 ps. In **DMAC–TRZ**, $I_{E,q\text{-copl.}}/I_{E,perp.}$ was estimated to be 13.9 immediately after photoexcitation and it decreased to 0.81 at 150 ps. In **PXZ–TRZ**, $I_{E,q\text{-copl.}}/I_{E,perp.}$ was estimated to be 1.5 immediately after photoexcitation and it decreased to 0.18 at 150 ps. These values of

Table 2 The values of $I_{E,q\text{-copl.}}/I_{E,perp.}$ obtained from the TR-PL spectra and $N_{q\text{-copl.}}/N_{perp.}$ calculated based on the Boltzmann distribution in the S_0 state

	$I_{E,q\text{-copl.}}/I_{E,perp.}$	$N_{q\text{-copl.}}/N_{perp.}$	$f_{q\text{-copl.}}/f_{perp.}$
PTZ–TRZ	141	2.9	47.9
DMAC–TRZ	13.9	0.085	164
PXZ–TRZ	1.5	0.012	123

$I_{E,q\text{-copl.}}/I_{E,perp.}$ immediately after photoexcitation are summarized in Table 2.

Given that the emission mechanism is the same for the three molecules, the emission intensity immediately after photoexcitation should be determined by the population in the S_0 state before photoexcitation. To estimate the population in the S_0 state, we first calculated the S_0 energies of the q-copl. conformer with respect to that of the perp. conformer (ΔE) for the three molecules by DFT calculations and the values are summarized in Fig. 5. The values of ΔE were −28 meV, 64 meV, and 114 meV in **PTZ–TRZ**, **DMAC–TRZ**, and **PXZ–TRZ**, respectively. Note that we confirmed that these values do not largely depend on the functional in the calculations (Table S3, ESI†). Because the less the energy of a state is, the more the state is populated in thermal equilibrium, this order of ΔE is consistent with the order of magnitude of the q-copl./perp. emission ratio immediately after photoexcitation in the dual emission. To confirm whether the two structures are in thermal equilibrium in the S_0 state, the potential energy surfaces along the D–A dihedral rotation of the three molecules in the S_0 state were calculated (Fig. S17, ESI†). The activation energy from the q-copl. to perp. conformer was 44–128 meV and that from the perp. to q-copl. conformer was 109–165 meV (Table S4, ESI†). These results indicate that the structural change over the activation energy can occur at room temperature. The stability of the q-copl. conformer is influenced by the fold angle of the donor plane and the bent angle of the donor with respect to the acceptor within the q-copl. conformer. Further details are provided in the ESI,† SI-8.

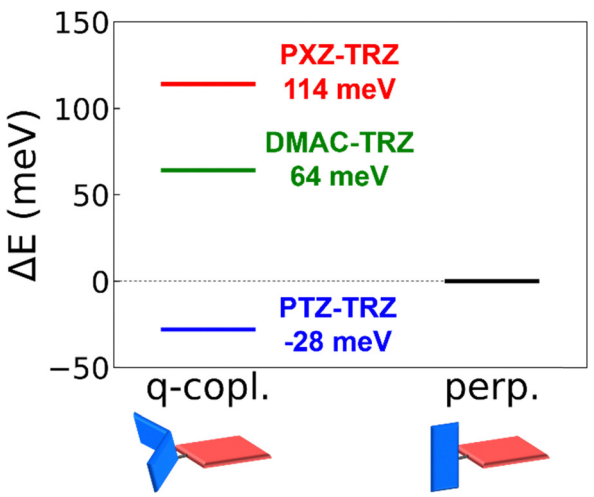

Fig. 5 The calculated S_0 energies of the q-copl. conformer with respect to that of the perp. conformer for **PTZ–TRZ**, **DMAC–TRZ** and **PXZ–TRZ**.

From the values of ΔE, we calculated the population ratio of the q-copl. and perp. conformers of the three molecules in the S_0 state. Based on the Boltzmann distribution, the ratio of their populations, $N_{q\text{-copl.}}/N_{perp.}$, can be expressed using the following equation:[28]

$$N_{q\text{-copl.}}/N_{perp.} = \exp\left(-\frac{\Delta E}{k_B T}\right) \quad (1)$$

where k_B is the Boltzmann constant and T is the temperature. At room temperature (300 K), the $N_{q\text{-copl.}}/N_{perp.}$ values were calculated to be 2.9 in **PTZ–TRZ**, 0.085 in **DMAC–TRZ** and 0.012 in **PXZ–TRZ**, as summarized in Table 2. This result suggests that the population in **PTZ–TRZ** is biased toward the q-copl. conformer, while that in **DMAC–TRZ** and **PXZ–TRZ** is predominantly biased toward the perp. conformer. Given that there is no other relaxation process immediately after photoexcitation, emission intensity (I_E) is proportional to the product of the molar absorption coefficient and population (N). Because the molar absorption coefficient is regarded to be proportional to oscillator strength, the ratio of oscillator strength, $f_{q\text{-copl.}}/f_{perp.}$, between the two conformers can be estimated from $I_{E,q\text{-copl.}}/I_{E,perp.}$ and $N_{q\text{-copl.}}/N_{perp.}$. The estimated values were 47.9, 164, and 123 for **PTZ–TRZ**, **DMAC–TRZ**, and **PXZ–TRZ**, respectively (summarized in Table 1). We found that the $f_{q\text{-copl.}}/f_{perp.}$ values were in agreement with those obtained by the quantum chemical calculations, as discussed in detail in the ESI,† SI-9. Thus, we concluded that the emission intensity ratio between the two conformers immediately after photoexcitation is determined by the difference in the population of the two conformers in the S_0 state.

TA spectra and their analyses

To confirm the early emission dynamics derived from the TR-PL spectra, the TA spectra of **PTZ–TRZ**, **DMAC–TRZ**, and **PXZ–TRZ** were measured in toluene solution, as shown in Fig. 6a, d and g, respectively. A common feature of the TA spectra of the three molecules is that the spectral intensity slightly increases as a function of delay time. Simultaneously, the spectral shape varies but the degree of variation depends on the molecule. **PTZ–TRZ**, with a higher population of the q-copl. conformer in the S_0 state, showed a significant change from the broad featureless spectrum to that with vibronic progression. **DMAC–TRZ** showed a similar trend but to a lesser extent, while **PXZ–TRZ** showed only minor changes. These trends can be more obviously seen in the normalized TA spectra shown in Fig. S19 (ESI†).

These results indicate that the higher the population of the q-copl. conformer in the S_0 state is, the more pronounced the spectral changes are. According to the emission mechanism proposed above, immediately after photoexcitation, the $^1LE_{q\text{-copl.}}$ and $^1CT_{perp.}$ states are simultaneously populated. Subsequently the $^1LE_{q\text{-copl.}}$ state undergoes relaxation to the $^1CT_{q\text{-copl.}}$ state with a time constant of 3–7 ps and structural relaxation to the $^1CT_{perp.}$ state. Based on this mechanism, the

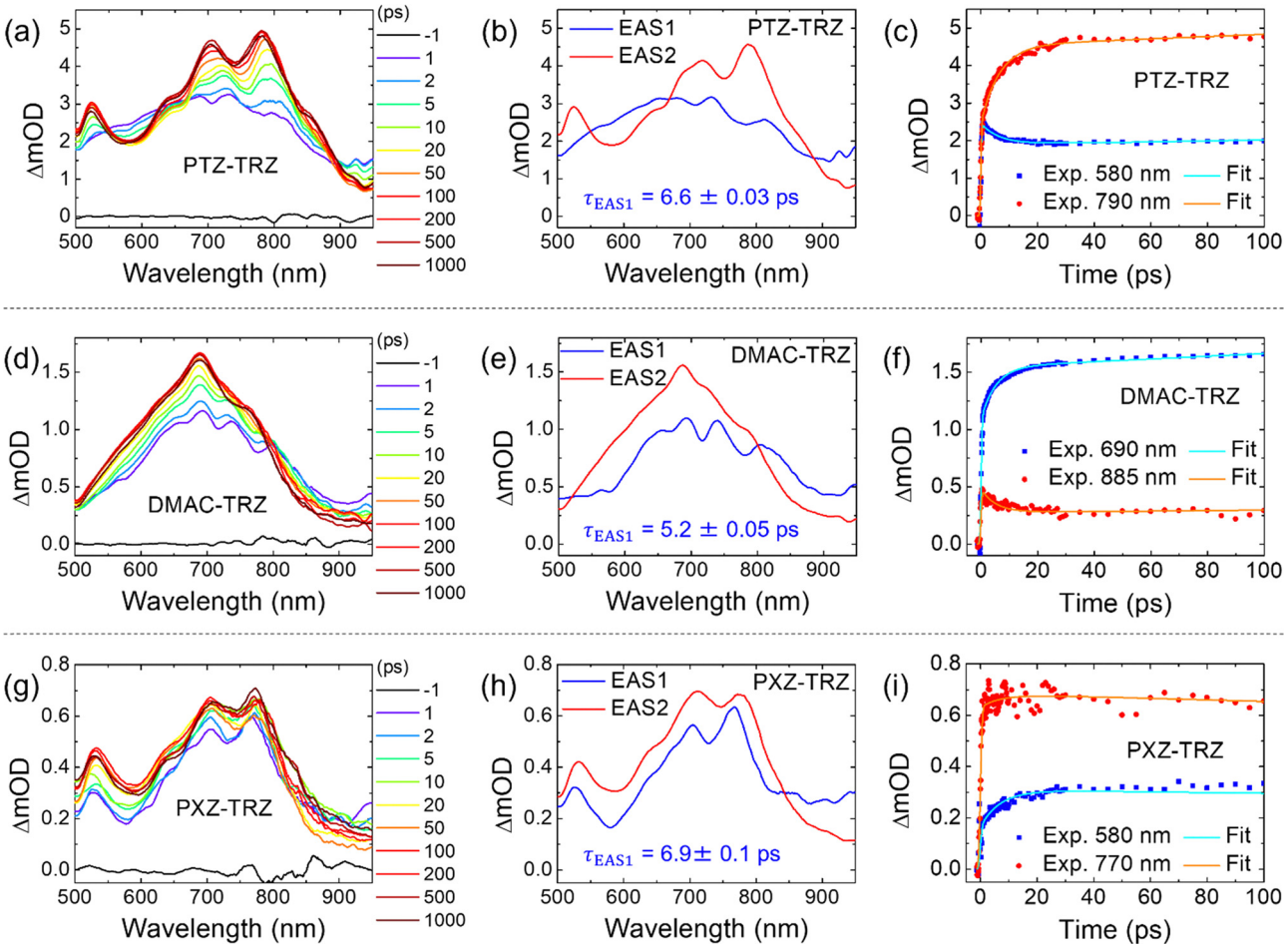

Fig. 6 The TA spectra of (a) **PTZ–TRZ**, (d) **DMAC–TRZ**, and (g) **PXZ–TRZ**. The excitation wavelengths were 360 nm for **PTZ–TRZ**, 370 nm for **DMAC–TRZ**, and 345 nm for **PXZ–TRZ**. The EAS of (b) **PTZ–TRZ**, (e) **DMAC–TRZ**, and (h) **PXZ–TRZ** derived from the TA spectra using a global analysis. Comparison of the time profiles of the TA spectra and the fitting of the global analysis for (c) **PTZ–TRZ** (580 and 790 nm), (f) **DMAC–TRZ** (690 and 885 nm), and (i) **PXZ–TRZ** (580 and 770 nm). The global analysis was conducted using a sequential two-state model for all the molecules.

broad spectra immediately after photoexcitation in the TA spectra are attributed to the coexistence of the $^1LE_{q\text{-copl.}}$ and $^1CT_{perp.}$ states, while the subsequent spectra with vibrational progression correspond to the coexistence of the $^1CT_{q\text{-copl.}}$ and $^1CT_{perp.}$ states. Furthermore, in all three molecules, the total area of each spectrum does not decrease up to 1 ns, indicating that the excited state decay is negligible on the sub-nanosecond timescale. This finding agrees well with the above conclusion that the fast decay of fluorescence for the q-copl. conformer is attributed to the decay from the high oscillator strength state ($^1LE_{q\text{-copl.}}$) to the almost zero oscillator strength state ($^1CT_{perp.}$) with respect to the S_0 state.

We conducted the global analysis of the time evolutions of the TA spectra up to 100 ps using a sequential two-state model based on the results of TR-PL and TA spectroscopy shown in Fig. S20 (ESI†). In this model, EAS1 was assigned to the coexistence state of the $^1LE_{q\text{-copl.}}$ and $^1CT_{perp.}$ states before structural relaxation, and EAS2 was assigned to the coexistence state of the $^1CT_{q\text{-copl.}}$ and $^1CT_{perp.}$ states after structural relaxation. The results of **PTZ–TRZ**, **DMAC–TRZ**, and **PXZ–TRZ** are shown in Fig. 6b, c, e, f, h and i, respectively. The spectral change from EAS1 to EAS2 was pronounced for **PTZ–TRZ** and **DMAC–TRZ**, and only slightly for **PXZ–TRZ**. The τ_{EAS1} values were 6.6 ps, 5.2 ps, and 6.9 ps for **PTZ–TRZ**, **DMAC–TRZ**, and **PXZ–TRZ**, respectively, and the τ_{EAS2} values were longer than 100 ps in all three molecules because the spectra had not fully decayed within the time window up to 100 ps. These results indicate that the time constant at which the dominant transient species transitions from the $^1LE_{q\text{-copl.}}$ and the $^1CT_{perp.}$ state before structural relaxation to the $^1CT_{q\text{-copl.}}$ and the $^1CT_{perp.}$ state after structural relaxation is 5–7 ps. These time constants are consistent with those estimated by TR-PL, corresponding to the relaxation from the $^1LE_{q\text{-copl.}}$ to the $^1CT_{q\text{-copl.}}$ state and the structural relaxation in the $^1CT_{perp.}$ state.

Dual emission mechanism common to the three molecules

The common dual emission mechanism we proposed here for all three molecules is depicted in Fig. 7. In the S_0 state, both q-copl. and perp. conformers coexist, and the ratio of their presence depends on the energetic stability of the q-copl. conformer. Upon UV irradiation, both conformers are excited to the higher excited state ((i) in Fig. 7). After that, in the q-copl.

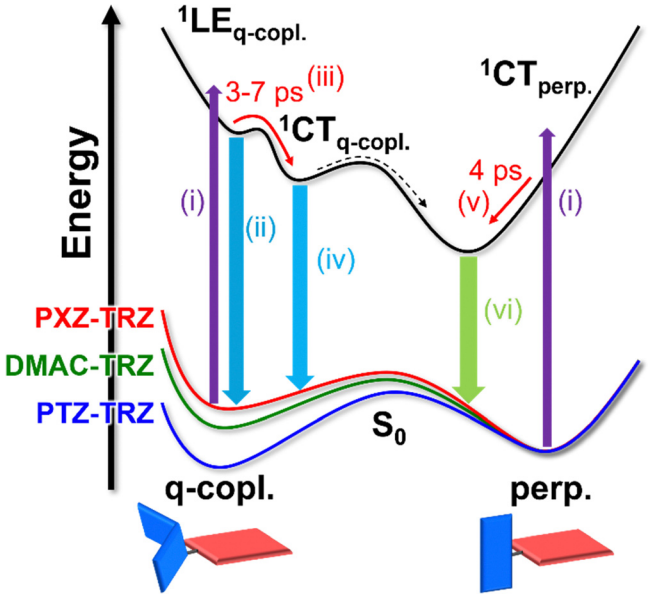

Fig. 7 The schematic of the proposed common emission mechanism for the three linearly-linked D–A molecules exhibiting dual emission: **PTZ–TRZ**, **DMAC–TRZ**, and **PXZ–TRZ**.

conformer, the $^1LE_{q\text{-}copl.}$ state (S_2 state) with high oscillator strength from the S_0 state is created and emits strong fluorescence centered at approximately 400 nm (ii). Simultaneously, internal conversion occurs to the $^1CT_{q\text{-}copl.}$ state (S_1 state) associated with vibrational relaxation and solvation with a time constant of 3–7 ps (iii). Subsequently, the $^1CT_{q\text{-}copl.}$ state emits weak fluorescence (iv). Fast PL decay within a few picoseconds indicates electronic and structural relaxation of the excited state as it acquires some CT character and its oscillator strength decreases. In the perp. conformer, after photoexcitation, the structural relaxation in the $^1CT_{perp.}$ state (S_1 state) occurs with a time constant of 4 ps (v). Then the $^1CT_{perp.}$ state with low oscillator strength emits long-lifetime fluorescence (vi). The emission intensity ratio between the q-copl. and perp. conformers is determined by the stability of the q-copl. conformer in the S_0 state. The structural change from the q-copl. conformer to the perp. conformer, which is reported in the previous studies, could not be clearly observed in our measurements. However, we cannot rule out the possibility that the structural change occurs along with the excited-state processes shown here.

Conclusions

We have investigated the dual emission mechanism in the three linearly-linked D–A type TADF molecules **PTZ–TRZ**, **DMAC–TRZ**, and **PXZ–TRZ** using picosecond TR-PL spectroscopy, femtosecond TA spectroscopy, and quantum chemical calculations. We found that not only **PTZ–TRZ** and **DMAC–TRZ** but also **PXZ–TRZ** exhibit dual emission in the steady-state PL spectra. The TR-PL spectra revealed that all three molecules more clearly exhibit dual emission in the picosecond region. In the q-copl. conformer, the emission exhibits a red shift as a function of delay time in all three molecules, which is attributed to the relaxation from the higher singlet excited state to the S_1 state. In contrast, in the perp. conformer, a red shift in the emission was observed only in **PXZ–TRZ**, which is attributed to the structural relaxation of the S_1 state. The quantum chemical calculations revealed that the higher excited state exhibiting fluorescence in the q-copl. conformer of each molecule was the $^1LE_{q\text{-}copl.}$ state (S_2 state). The time constant of the relaxation to the $^1CT_{q\text{-}copl.}$ state (S_1 state) in the q-copl. conformer is 3–7 ps and that of structural relaxation in the $^1CT_{perp.}$ state (S_1 state) in the perp. conformer is 4 ps. The emission intensity of the q-copl. conformer immediately after photoexcitation relative to that of the perp. conformer is determined by the population ratio of the two conformers in the S_0 state. The TA spectra of the three molecules changed with a time constant of 5–7 ps, accompanied by varying degrees of change for each molecule. These changes are assigned to the relaxation from the mixed state of the $^1LE_{q\text{-}copl.}$ and $^1CT_{perp.}$ states to the mixed state of the $^1CT_{q\text{-}copl.}$ and $^1CT_{perp.}$ states. The dual-emission mechanism we proposed here is presumably applicable to other linearly-linked D–A type TADF molecules. These studies have revealed the previously overlooked photophysical properties of D–A molecules through a detailed analysis of their physical properties using spectroscopic techniques. Our findings provide a more profound comprehension of the photophysical properties of D–A molecules and underscore the significance of meticulous spectroscopic analysis in elucidating intricate excited-state dynamics. These insights pave the way for the development of new types of photofunctional materials.

Author contributions

K. O. conceived and supervised the project. T. R. contributed to conceptualization, methodology, investigation, and writing the original draft. M. S. investigated the data. K. M. contributed to conceptualization, methodology, and investigation. A. R. and I. S. provided instruments and contributed to conceptualization and investigation. Y. T., H. N. and C. A. prepared all molecules. All authors contributed to the review and editing of the manuscript and critically commented on the project.

Conflicts of interest

There are no conflicts to declare.

Data availability

The data supporting this article have been included as part of the ESI and are also available at the link given in the ESI.†

Acknowledgements

This work was partially supported by JSPS KAKENHI Grant Numbers JP23H01977, JP23H04631, JP23K20039, and JP24KJ1791. The work at the University of St Andrews was supported by the

Engineering and Physical Sciences Research Council of the UK through grant ER/R035164/1. We acknowledge Prof. Nobuhiro Yanai at Kyushu University for the measurement of UV-vis absorption spectra.

References

1 H. Uoyama, K. Goushi, K. Shizu, H. Nomura and C. Adachi, Highly efficient organic light-emitting diodes from delayed fluorescence, *Nature*, 2012, **492**, 234–238.
2 V. Jankus, P. Data, D. Graves, C. McGuinness, J. Santos, M. R. Bryce, F. B. Dias and A. P. Monkman, Highly efficient TADF OLEDs: How the emitter–host interaction controls both the excited state species and electrical properties of the devices to achieve near 100% triplet harvesting and high efficiency, *Adv. Funct. Mater.*, 2014, **24**, 6178–6186.
3 Y. Kitamoto, T. Namikawa, D. Ikemizu, Y. Miyata, T. Suzuki, H. Kita, T. Sato and S. Oi, Light blue and green thermally activated delayed fluorescence from 10 H -phenoxaborin-derivatives and their application to organic light-emitting diodes, *J. Mater. Chem. C*, 2015, **3**, 9122–9130.
4 H. Peng, Y. Xu, C. Zhou, R. Pei, J. Miao, H. Liu and C. Yang, Donor extension on Spiro-acridine enables highly efficient TADF-OLEDs with relieved efficiency roll-off, *Adv. Funct. Mater.*, 2023, **33**, 2211696.
5 W. Chen, S. Xu, J. J. Day, D. Wang and M. Xian, A general strategy for development of near-infrared fluorescent probes for bioimaging, *Angew. Chem.*, 2017, **129**, 16838–16842.
6 X. Zhang, T. Ren, F. Yang and L. Yuan, Rational design of far red to near-infrared rhodamine analogues with huge Stokes shifts for single-laser excitation multicolor imaging, *Chin. Chem. Lett.*, 2021, **32**, 3890–3894.
7 H. Li, Y. Shen, Z. Dong, W. Li and L. Yuan, Rational design of tunable near-Infrared oxazine probe with large Stokes shift for leucine aminopeptidase detection and imaging, *Chem. – Asian J.*, 2023, **18**, e202300701.
8 H. Hu, P. C. Y. Chow, G. Zhang, T. Ma, J. Liu, G. Yang and H. Yan, Design of Donor Polymers with Strong Temperature-Dependent Aggregation Property for Efficient Organic Photovoltaics, *Acc. Chem. Res.*, 2017, **50**, 2519–2528.
9 L. Zhu, M. Zhang, J. Xu, C. Li, J. Yan, G. Zhou, W. Zhong, T. Hao, J. Song, X. Xue, Z. Zhou, R. Zeng, H. Zhu, C.-C. Chen, R. C. I. MacKenzie, Y. Zou, J. Nelson, Y. Zhang, Y. Sun and F. Liu, Single-junction organic solar cells with over 19% efficiency enabled by a refined double-fibril network morphology, *Nat. Mater.*, 2022, **21**, 656–663.
10 K. Wang, C.-J. Zheng, W. Liu, K. Liang, Y.-Z. Shi, S.-L. Tao, C.-S. Lee, X.-M. Ou and X.-H. Zhang, Avoiding energy loss on TADF emitters: Controlling the dual conformations of D–A structure molecules based on the pseudoplanar segments, *Adv. Mater.*, 2017, **29**, 1701476.
11 W. Li, X. Cai, B. Li, L. Gan, Y. He, K. Liu, D. Chen, Y.-C. Wu and S.-J. Su, Adamantane-substituted acridine donor for blue dual fluorescence and efficient organic light-emitting diodes, *Angew. Chem.*, 2019, **131**, 592–596.
12 D. de Sa Pereira, D. R. Lee, N. A. Kukhta, K. H. Lee, C. L. Kim, A. S. Batsanov, J. Y. Lee and A. P. Monkman, The effect of a heavy atom on the radiative pathways of an emitter with dual conformation, thermally-activated delayed fluorescence and room temperature phosphorescence, *J. Mater. Chem. C*, 2019, **7**, 10481–10490.
13 K. Wang, Y.-Z. Shi, C.-J. Zheng, W. Liu, K. Liang, X. Li, M. Zhang, H. Lin, S.-L. Tao, C.-S. Lee, X.-M. Ou and X.-H. Zhang, Control of Dual Conformations: Developing Thermally Activated Delayed Fluorescence Emitters for Highly Efficient Single-Emitter White Organic Light-Emitting Diodes, *ACS Appl. Mater. Interfaces*, 2018, **10**, 31515–31525.
14 S. Xiang, R. Guo, Z. Huang, X. Lv, S. Sun, H. Chen, Q. Zhang and L. Wang, Highly efficient yellow nondoped thermally activated delayed fluorescence OLEDs by utilizing energy transfer between dual conformations based on phenothiazine derivatives, *Dyes Pigm.*, 2019, **170**, 107636.
15 X. Song, S. Shen, M. Lu, Y. Wang and Y. Zhang, Trifluoromethyl enable high-performance single-emitter white organic light-emitting devices based on quinazoline acceptor, *Chin. Chem. Lett.*, 2024, **35**, 109118.
16 X. Tian, S. Xiao, J. Sun, J. Yan, G. Li, B. Zhao, Y. Miao, L. Wang, H. Wang and D. Ma, Dual fluorescence induced thermally activated delayed fluorescence materials based on 2,4-Diphenylthieno[3,2-d]pyrimidine with an efficient single-molecular white electroluminescence, *Chem. Eng. J.*, 2024, **485**, 149692.
17 H. Tanaka, K. Shizu, H. Nakanotani and C. Adachi, Dual Intramolecular Charge-Transfer Fluorescence Derived from a Phenothiazine–Triphenyltriazine Derivative, *J. Phys. Chem. C*, 2014, **118**, 15985–15994.
18 K. Stavrou, L. G. Franca, T. Böhmer, L. M. Duben, C. M. Marian and A. P. Monkman, Unexpected quasi-axial conformer in thermally activated delayed fluorescence DMAC-TRZ, pushing green OLEDs to blue, *Adv. Funct. Mater.*, 2023, **33**, 202300910.
19 D.-G. Chen, T.-C. Lin, Y.-A. Chen, Y.-H. Chen, T.-C. Lin, Y.-T. Chen and P.-T. Chou, Revisiting Dual Intramolecular Charge-Transfer Fluorescence of Phenothiazine–triphenyltriazine Derivatives, *J. Phys. Chem. C*, 2018, **122**, 12215–12221.
20 T. Ryu, K. Miyata, M. Saigo, Y. Shimoda, Y. Tsuchiya, H. Nakanotani, C. Adachi and K. Onda, Solvent-dependent dual emission processes in charge-transfer excited states of phenothiazine–triphenyltriazine conformers, *Chem. Phys. Lett.*, 2022, **809**, 140155.
21 L. G. Franca, A. Danos, R. Saxena, S. Kuila, K. Stavrou, C. Li, S. Wedler, A. Köhler and A. P. Monkman, Exploring the Early Time Behavior of the Excited States of an Archetype Thermally Activated Delayed Fluorescence Molecule, *J. Phys. Chem. Lett.*, 2024, **15**, 1734–1740.
22 H. Tanaka, K. Shizu, H. Miyazaki and C. Adachi, Efficient green thermally activated delayed fluorescence (TADF) from a phenoxazine–triphenyltriazine (PXZ–TRZ) derivative, *Chem. Commun.*, 2012, **48**, 11392–11394.
23 W.-L. Tsai, M.-H. Huang, W.-K. Lee, Y.-J. Hsu, K.-C. Pan, Y.-H. Huang, H.-C. Ting, M. Sarma, Y.-Y. Ho, H.-C. Hu,

C.-C. Chen, M.-T. Lee, K.-T. Wong and C.-C. Wu, A versatile thermally activated delayed fluorescence emitter for both highly efficient doped and non-doped organic light emitting devices, *Chem. Commun.*, 2015, **51**, 13662–13665.

24 J. J. Snellenburg, S. Laptenok, R. Seger, K. M. Mullen and I. H. M. van Stokkum, Glotaran: A Java-Based Graphical User Interface for the R Package TIMP, *J. Stat. Softw.*, 2012, **49**, 1–22.

25 M. J. Frisch, G. W. Trucks, H. B. Schlegel, G. E. Scuseria, M. A. Robb, J. R. Cheeseman, G. Scalmani, V. Barone, G. A. Petersson, H. Nakatsuji *et al.*, *Gaussian 16, Revision C.01*, 2016, Gaussian Inc., Wallingford CT.

26 Y. Shimoda, K. Miyata, M. Saigo, Y. Tsuchiya, C. Adachi and K. Onda, Intramolecular-rotation driven triplet-to-singlet upconversion and fluctuation induced fluorescence activation in linearly connected donor-acceptor molecules, *J. Chem. Phys.*, 2020, **153**, 204702.

27 P. Changenet, P. Plaza, M. M. Martin and Y. H. Meyer, Role of intramolecular torsion and solvent dynamics in the charge-transfer kinetics in triphenylphosphine oxide derivatives and DMABN, *J. Phys. Chem. A*, 1997, **101**, 8186–8194.

28 S. A. C. McDowell, A simple derivation of the Boltzmann distribution, *J. Chem. Educ.*, 1999, **76**, 1393.

